INTERNATIONAL JOURNAL OF OPTIMIZATION IN CIVIL ENGINEERING
Int. J. Optim. Civil Eng., 2022; 12(4): 577-594

THE EFFECT OF BLAST POSITIVE IMPACT DURATION ON THE MAXIMUM RESPONSES OF A NONLINEAR DYNAMIC SYSTEM

R. Kamgar[1*, †], R. Alipour[2] and S. Rostami[3]
[1]*Department of Civil Engineering, Shahrekord University, Shahrekord, Iran*
[2]*Department of Civil Engineering, Shahrekord University, Shahrekord, Iran*
[3]*Department of Civil Engineering, Technical and Vocational University, Tehran, Iran*

ABSTRACT

Explosions are inevitable in today's world; therefore, building structures may be dynamically loaded by an intense loading during the explosion. This is why regulatory bodies have provided instructions for determining the response of structures under the explosion load. Previous research has shown that when the explosion happens close to a structure, the ground explosion load can be modeled as tensile and compressive loads. This research investigates the response of an elastic-plastic single-degree-of-freedom system subjected to different explosive loads with different positive durations. The maximum intensity of blast load and blast duration remains constant, and the positive phase duration is the only variable that changes. The nonlinear dynamic responses of a single-degree-of-freedom system (i.e., displacement, velocity, acceleration, and ductility) are calculated using the linear acceleration method. The results show that increasing the positive phase duration and the amount of positive impact can increase the maximum displacement and ductility of the system. Also, it can be concluded that the maximum acceleration of the studied systems remains constant when the values for the blast impact and positive phase durations change.

Keywords: Blast; Nonlinear dynamic analysis; Elastic-Plastic model; Strain hardening; Impact

Received: 5 July 2022; Accepted: 24 August 2022

1. INTRODUCTION

Research has recently been conducted on modeling the loads caused by earthquakes and explosions on objects and structures [1-8]. The design and analysis of structures under

[*]Corresponding author: Department of Civil Engineering, Shahrekord University, Shahrekord, Iran
[†]E-mail address: kamgar@sku.ac.ir (R. Kamgar)

explosion load require an accurate understanding of the explosion phenomenon and the dynamic response of structural elements under blast load. Some researchers, such as Ref. [9], have studied the effect of explosion load on structures in detail. In this reference, the nature of the explosion, the mechanism of explosion waves in the open air, and different methods for estimating the explosion load and the response of the structure have been investigated. Under the blast load, the structures enter the nonlinear zone, and it can maximize the amount of energy loss with ductile behavior.

In the dynamic analysis using numerical methods, the structure's response under external load can be calculated using direct integration methods. These numerical methods are divided into explicit [10-13] and implicit methods [14-17]. If the system's equation of motion is used at any time step to determine displacement at the same time step, the method is implicit; otherwise, the method is explicit. In other words, in the explicit integration method, the unknown values of displacement $x_{t+\Delta t}$, velocity $\dot{x}_{t+\Delta t}$, and acceleration $\ddot{x}_{t+\Delta t}$ for the time step $t+\Delta t$, are obtained using the equilibrium conditions at time t and the known values $\dot{x}_t, x_t$, and $\ddot{x}_t$. However, in the implicit method, the unknown values $x_{t+\Delta t}$ ، $\dot{x}_{t+\Delta t}$, $\ddot{x}_{t+\Delta t}$, are calculated using the equilibrium conditions in time $t+\Delta t$.

In contrast, explicit methods involve solving a series of linear equations so that they contain only one unknown value. Therefore, explicit methods do not need to decompose the coefficient matrix (a combination of stiffness, mass, and damping matrices). These methods store the solution of the equation of motion for a model of a discrete multi-degree-of-freedom system as the step-by-step [18]. The most important advantages of explicit integration methods over implicit methods are less computational effort and fewer data storage per step.

In contrast, the most important drawback of such methods is that almost all of them are conditionally stable. This shortcoming subsequently causes a smaller time step and, consequently, an increase in the number of steps in the analysis [19-20]. According to published literature, implicit algorithms are more effective in solving structural dynamics problems in which several low-frequency modes control the structural response. On the other hand, explicit algorithms have high efficiency in wave propagation problems in which the participation of medium and high-frequency structural modes is important [21-22]. In general, of these two types of numerical methods, implicit methods are more common in earthquake problems due to their ability to use larger time steps.

On the other hand, explicit methods have also been considered due to their greater accuracy and lower computational cost. In explosion problems, small-time steps in the analysis process are required to determine the response of a structure in real dimensions, which includes thousands of degrees of freedom. Implicit methods are more computationally impractical than explicit ones. The explicit Newmark method, the central difference method, and the explicit Rang-Kota method are common examples of these methods. In addition, since implementing an explicit method for performing quasi-realistic dynamic experiments is simpler than an implicit method, explicit methods are more appropriate for conducting such experiments [10, 23]. This paper investigates the response of a single-degree-of-freedom system with an elastic-plastic nonlinear behavioral model under explosion load with different positive impact times. In this paper, it assumes that the maximum blast load and blast duration remain constant. In contrast, only the duration of the positive impact

changes. The results also show that for different positive impact times, the maximum acceleration of the studied system remains constant under the explosion's impact.

An *explosion* is the release of sudden, rapid, and large-scale energy. The explosion inside or near a structure has catastrophic and destructive effects. Explosions are classified into physical, nuclear, and chemical according to their physical nature. In a physical explosion, energy may be released from the collapse of a gas-pressed cylinder, a volcanic eruption, or the mixing of two liquids at different temperatures. In the nucleus explosion, the nuclear formation of different atoms and redistribution of neutrons and protons occurs in nuclear interactions.

In contrast, the main energy source is the rapid oxidation of fuel components (hydrogen and carbon atoms) in a chemical explosion [24]. Explosive materials are classified into three categories based on their physical state: liquid, solid, and gas. Solid explosives are very sensitive to heat and can be classified according to their sensitivity to combustion to primary and secondary explosives. Explosives are easily detonated with a flame or blow. In secondary explosives, the explosion produces a wave that causes damage to the surroundings. Materials such as TNT, ammonium nitrate, and furnace oil are in this category [24]. The explosion of compressed explosives produces hot gases under pressure above 300 *kbar* and temperatures above 3000 ^{0}C to 4000 ^{0}C. In this case, the hot gas expands and takes up more space. As a result, a layer of compressed air (blast wave) is formed in front of this volume of gas, which contains most of the energy released from the explosion [24].

The resulting blast wave increases to a pressure greater than the ambient pressure. This pressure is attributed to high pressure and develops as an explosion wave outside the source of the explosion and decreases in intensity over time. After a short time, the pressure behind the wavefront may be reduced to ambient pressure (Figs. 1-2). Meanwhile, a small vacuum forms and sucks air in. This is accompanied by high suction winds that carry debris for long distances away from the source of the explosion. In other words, the blast wave is caused by a rapid increase in air pressure from the atmospheric point to the explosion's peak pressure, followed by a rapid decrease in atmospheric pressure and then a gradual increase in atmospheric pressure. Therefore, the blast wave has two phases. The rapid increase in pressure that leads to an increase in atmospheric pressure, known as the positive phase or the compression phase, and the decrease in pressure to the atmospheric level, which results in a return to the atmospheric state, is called the negative phase or the suction phase. At a certain distance from the blast site, after a short time, the pressure of that blast suddenly rises until it reaches its peak. After that, the pressure gradually decreases to ambient pressure and even lower values [24-26].

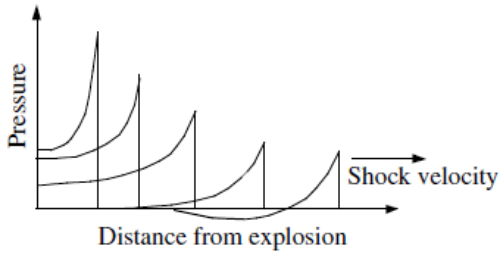

Figure 1. Explosion wave propagation [24]

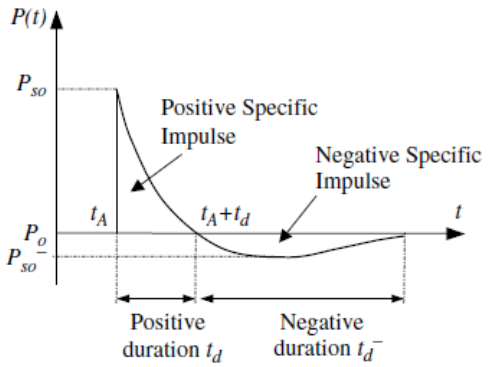

Figure 2. The explosion wave pressure-time history [24]

In Fig. 2, the area below the time-pressure curve in the interval of t_A to $t_A + t_d$ seconds is called the positive shock of the explosion, which can be calculated as follows [24]:

$$i_s = \int_{t_A}^{t_A+t_d} p_{so}(t)\, dt \tag{1}$$

Two important components define the behavior of a conventional bomb: 1- the size of the bomb or the weight of the charge W and 2- the distance between the source of the explosion and the target R (Fig. 3).

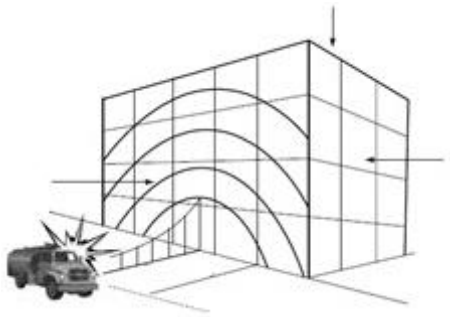

Figure 3. Explosive loads on a building [24]

Recently, several studies on the effect of the explosion on the dynamic response of the structure have been conducted by researchers [27-31]. For example, Magnesa and Morel [32] conducted experimental studies on concrete beams with different strengths under blast load. This study aimed to investigate how the load is transferred to the supports for a single-degree of freedom system. Bahiraei et al. [33] also investigated the effect of the explosion on the response of concrete slabs using ANSYS software. Habibi and Khaledi [34] investigated the nonlinear response of composite bridges under explosion load. In another study, Khaledi et al. [35-36] studied the weight minimization and drift of the bending frame

to optimize the design of structures under explosion load. They optimized the sections that brought the minimum weight for the structure and met the design criteria.

Recently, researchers have investigated the methods to reduce the response of structures under the explosion load. Mondel et al. [37] investigated the reduction in the response of a structure controlled by a viscous damper. In another study, Mendal et al. [38] investigated the performance of controlled structures using elastomeric and frictional seismic separators under underground blast load. The results showed that the acceleration and displacement values of the structure could be significantly reduced by using the studied separators. Kongda and Bakra [39] also investigated reducing the response of a structure controlled by a rubber core separator under explosion and earthquake loads. The results showed a large reduction in the acceleration and drift of the stories affected by the earthquake in a structure controlled by the rubber separator with the lead core. They also showed that as the yield strength increased, the separation displacement and the absolute acceleration of the roof decreased. In another study, Zhang and Phillips [40] examined the response of an isolated structure subjected to an explosion. Their research showed a reduction in drift stories and the absolute values of the story acceleration under the blast load.

In general, reinforced concrete structures suffer from brittle fractures in the event of high-velocity explosive loading. Therefore, most studies have focused on understanding the damage mechanisms and material behaviors of reinforced concrete structures under high-velocity explosive loads [41]. Gholipour et al. studied the investigation of rupture behavior and dynamic responses of reinforced concrete columns under the combination of impact load and explosion. They showed that the combination of impact load with far-field explosion leads to more severe damage. Their research also showed that the priority of impact loading instead of explosion provides more critical combined loading scenarios and causes more severe damage to the column [42]. Peymani Foroushani and Hosseini investigated the maximum deflection of a two-sided reinforced concrete slab under an explosion load. They presented an analytical method based on solving a single-degree-of-freedom system to calculate the deflection value of a two-sided slab [43].

2. RESEARCH METHODS

In this section, the pressure due to the explosion is expressed. All explosion parameters depend on the amount of energy released by the explosion, the waveform of the explosion, and the distance from the explosion site. According to a general definition, the effects of an explosion are expressed by a scaled distance that depends on $(E/P_0)^{1/3}$ and the scale pressure, such that E is the energy released in terms of (Kj) and P_0 is the ambient pressure (usually 100 kN/m^2). For simplicity, it is common to express the weight as an equivalent mass of TNT [24]. Explosion uses a law called scaled distance, which is used to find other parameters. The amount of pressure and impact released by the explosion on the structure can be calculated with empirical formulas obtained according to the law of scaled distance.

The approximation of the maximum pressure created in the explosion is expressed in terms of the scaled distance $Z = \frac{R}{W^{\frac{1}{3}}}$ by Brad with Eq. (2) as follows:

$$P_{SO} = \frac{6.7}{Z^3} + 1 \quad (P_{SO} \geq 10 \text{ bar})$$
$$P_{SO} = \frac{0.975}{Z} + \frac{1.455}{Z^2} + \frac{5.85}{Z^3} - 0.019 \quad (2)$$
$$(0.1 \text{ bar} \leq P_{SO} \leq 10 \text{ bar})$$

where R and W show the distance of the explosion charge to the desired location and the weight in terms of TNT weight, respectively. Henrich also presented Eq. (3) to calculate the maximum pressure load induced by the explosion [2]:

$$P_{SO} = \frac{14.072}{Z} + \frac{5.54}{Z^2} + \frac{0.357}{Z^3} + \frac{0.00625}{Z^4};$$
$$(0.05 \leq Z < 0.3)$$
$$P_{SO} = \frac{6.194}{Z} + \frac{0.326}{Z^2} + \frac{2.132}{Z^3}; \quad (3)$$
$$(0.3 \leq Z < 1)$$
$$P_{SO} = \frac{0.662}{Z} + \frac{4.05}{Z^2} + \frac{3.288}{Z^3};$$
$$(1 \leq Z < 10)$$

Brad's equations are well adapted to the experimental results for the distances far from the source of the explosion. In contrast, Henrich's equations are well adapted to the experimental results for the explosion of the near field. For this reason, short distances $Z \leq 0.5$ should use the Henrich equations, and in the middle distances and far from $Z > 0.5$, the results of Brad's equations are utilized [2]. The time history of blast wave pressure is often expressed by exponential functions such as the Freelander equation as follows [24]:

$$P(t) = P_o + P_{so}\left(1 - \frac{t}{t_d}\right)e^{\left(-b\frac{t}{t_d}\right)} \quad (4)$$

where t, P_o, P_{so}, t_d, and b are the time, the atmospheric pressure, the maximum overpressure, the positive phase time, and a positive number, respectively. Also, b is called the waveform parameter or the rate of pressure drop delay coefficient and is dependent on the maximum pressure [25].

In Eq. (4), t is in the unit of second. Also, P_{so} and P are defined in the unit of kPa.

Eq. (5) shows the equilibrium equation of an inelastic system:

$$[M]\{\ddot{x}\} + [C]\{\dot{x}\} + \{f_S(x)\} = \{P(t)\} \tag{5}$$

where *[M]* and *[C]* show the mass and damping matrices of the structure. The vectors $\{x\}, \{\dot{x}\}, \{\ddot{x}\}$, and $\{P(t)\}$ are the displacement, velocity, acceleration, and external forces vectors, respectively.

For a single degree of freedom system, matrices and vectors in Eq. (5) are converted to scalar values. Also, Eq. (5) can be solved numerically step-by-step. Some numerical methods such as Newmark β, Wilson-θ, central difference, Rang-Kota, Hobolt, and α-methods can be used for this purpose [42-43].

In this paper, the linear Newton-Raphson integration method is used. It is assumed that the structure's response exists in time t_i , and its response in time $t_{i+1} = t_i + \Delta t$ should be computed. Eq. (6) shows the equilibrium equation of a single-degree of freedom system with nonlinear behavior in an incremental form:

$$m\Delta\ddot{x}_i + c\Delta\dot{x}_i + \Delta f_{S_i} = \Delta P_i \tag{6}$$

where

$$\Delta f_{S_i} = k_i \Delta x_i \tag{7}$$

where k_i shows the tangential stiffness of the system at time t_i. Eqs. (6-7) are written as follows, considering the linear acceleration numerical integration method:

$$\hat{k}_i \, \Delta x^j{}_i = \Delta\hat{P}_i \tag{8}$$

In which

$$\begin{aligned} \hat{k}_i &= \frac{6}{\Delta t^2} m + \frac{3}{\Delta t} c + k_i \\ \Delta\hat{P}_i &= \Delta P(t) + \frac{6}{\Delta t} m\,\dot{x}_i + 3\,m\,\ddot{x}_i + 3\,c\,\dot{x}_i + \frac{\Delta t}{2} c\ddot{x}_i \end{aligned} \tag{9}$$

Eq. (8) is nonlinear because the tangential stiffness of the system depends on the displacement x_i ; therefore, the slope k_i is not constant. Here, Newton-Raphson's iteration process is used to solve this problem. In each iteration (*j*), the evolution of the displacement $\Delta x^j{}_i$ ، , the actual force $\Delta f^j{}_i$, which is less than $\Delta\hat{P}_i$, and therefore the force remaining in ($\Delta R^j{}_i$) can be calculated as follows:

$$\Delta R^j{}_i = \Delta\hat{P}_i - \Delta f^j{}_i \tag{10}$$

The incremental displacement Δx_i^j is used to determine a new value for the residual force, and the iteration process continues until the convergence criterion $\frac{\Delta x_i^l}{\sum_{n=1}^{l} \Delta x_i^n} \leq 0.001$ is reached.

By calculating the incremental displacement (Δx_i), the incremental velocity ($\Delta \dot{x}$), the incremental acceleration ($\Delta \ddot{x}$), the displacement, velocity, and acceleration are calculated as follows:

$$\begin{aligned}
\{\Delta \dot{x}_i\} &= \frac{3}{\Delta t}\{\Delta x_i\} - 3\{\dot{x}_i\} - \frac{\Delta t}{2}\{\ddot{x}_i\} \\
\{\Delta \ddot{x}_i\} &= \frac{6}{\Delta t^2}\{\Delta x_i\} - \frac{6}{\Delta t}\{\dot{x}_i\} - 3\{\ddot{x}_i\} \\
\{x_i\} &= \{x_i\} + \{\Delta x_i\} \\
\{\dot{x}_i\} &= \{\dot{x}_i\} + \{\Delta \dot{x}_i\} \\
\{\ddot{x}_i\} &= \{\ddot{x}_i\} + \{\Delta \ddot{x}_i\}
\end{aligned} \tag{11}$$

3. RESULTS AND DISCUSSION

Here, a single-degree of freedom system with mass equal to $m = 2.485 \times 10^5$ $(N.sec^2/m)$, stiffness equal to $m = 9.81 \times 10^6$ (N/m), and damping ratio equal to $\xi =$ 0.05 is considered. The yield displacement of the system is equal to 0.0075 *m*. Also, the explosion load applied to the system is considered $P(t) = 98100 \times (1 - \frac{2t}{3}) \times e^{-(\frac{5t}{6})}$ in the unit of *N* (see Fig. 4). The duration of the positive impact is $t_d = 1.5$ (sec). For this case, the positive impact of the load is equal to $5.0526 \times 10^4 (N.sec)$.

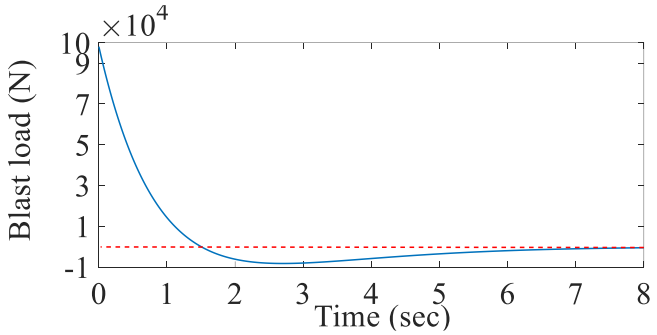

Figure 4. The time history of blast load with $t_d = 1.5$ (*sec*)

For the first time, the system is subjected to the blast load (see Fig. 4) with full elastic-plastic behavior (i.e., the strain hardening is not considered). In all analyses, the time step Δt is considered equal to 0.005 *sec*. Fig. 5 shows the acceleration, velocity, and displacement time histories of this system.

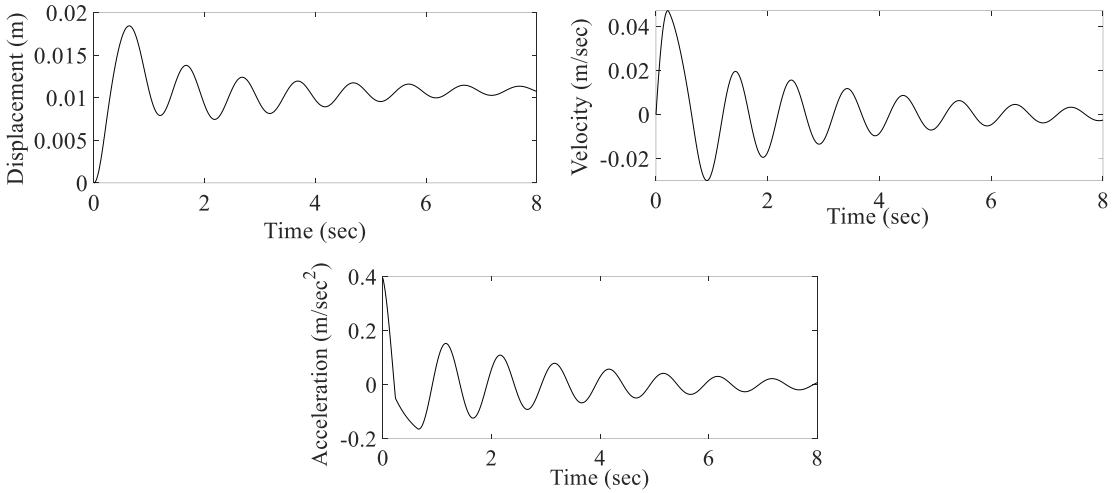

Figure 5. The displacement, velocity, and acceleration time histories of the system with full elastic-full plastic behavior subjected to the blast load with $t_d = 1.5$ (*sec*)

According to Fig. 5, the maximum displacement, velocity, and acceleration are equal to 0.0184 (*m)*, 0.041 (*m/sec*) and 0.3948 (*m/sec*^{2}), respectively. Also, the maximum ductility value is equal to $\mu = \frac{x_{max}}{x_y} = 2.46$. Also, Fig. 6 depicts the internal force concerning the displacement of the studied system.

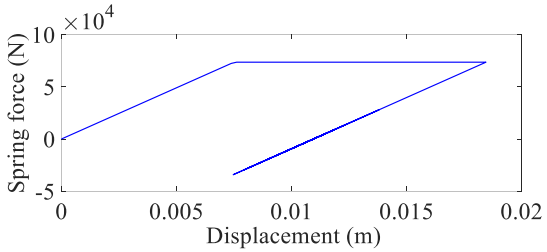

Figure 6. The change of internal force with respect to the displacement of the system subjected to the blast load with $t_d = 1.5$ (*sec*)

For the next state, the system is subjected to the blast load (see Fig. 7) with full elastic-plastic behavior (i.e., the strain hardening is not considered). Also, the explosion load applied to the system is considered $P(t) = 98100 \times (1 - 2t) \times e^{-(\frac{5t}{6})}$ in the unit of *N* (see Fig. 7). The duration of the positive impact is $t_d = 0.5$ (sec). For this case, the positive impact of the

load is equal to $2.1446\times10^{4}(N.sec)$. Fig. 8 shows the acceleration, velocity, and displacement time histories of this system.

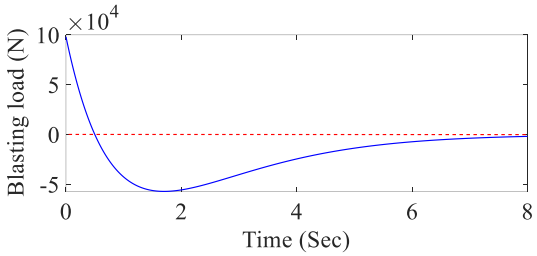

Figure 7. The time history of blast load with $t_d = 0.5$ (sec)

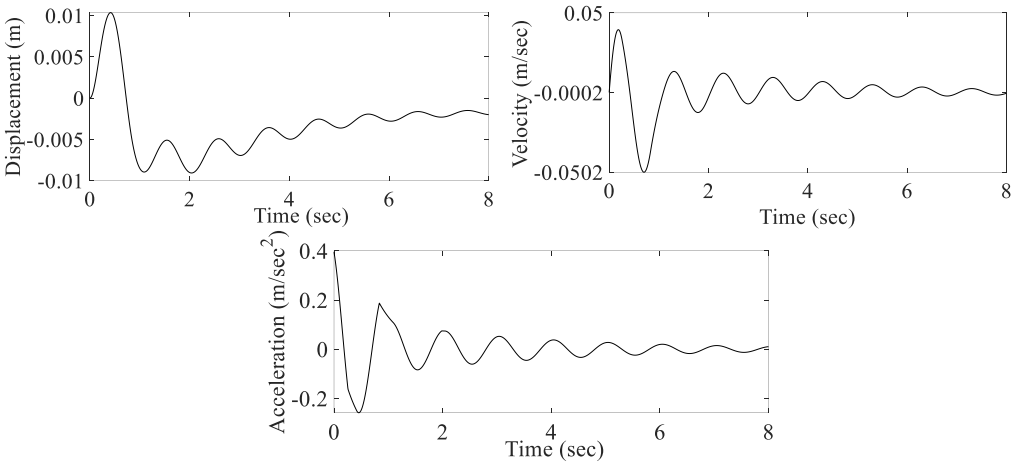

Figure 8. The displacement, velocity, and acceleration time histories of the system with full elastic-full plastic behavior subjected to the blast load with $t_d = 0.5$ (sec)

According to Fig. 8, the maximum displacement, velocity, and acceleration are equal to 0.0103 (m), 0.0502 (m/sec) and 0.3948 (m/sec^2), respectively. Also, the maximum ductility value is equal to $\mu = \frac{x_{max}}{x_y} = 1.38$. Also, Fig. 9 depicts the internal force concerning the displacement of the studied system.

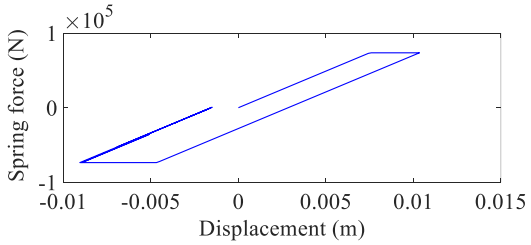

Figure 9. The change of internal force with respect to the displacement of the system subjected to the blast load with $t_d = 0.5$ (sec)

For the next state, the system is subjected to the blast load with full elastic-plastic behavior (i.e., strain hardening is not considered). Also, the explosion load applied to the system is considered $P(t) = 98100 \times (1 - \frac{t}{5}) \times e^{-(\frac{5t}{6})}$ in the unit of *N*. The duration of the positive impact is $t_d = 5\,(\text{sec})$. For this case, the positive impact of the load is equal to $8.9905 \times 10^4 (N.sec)$. Fig. 10 shows the acceleration, velocity, and displacement time histories of this system.

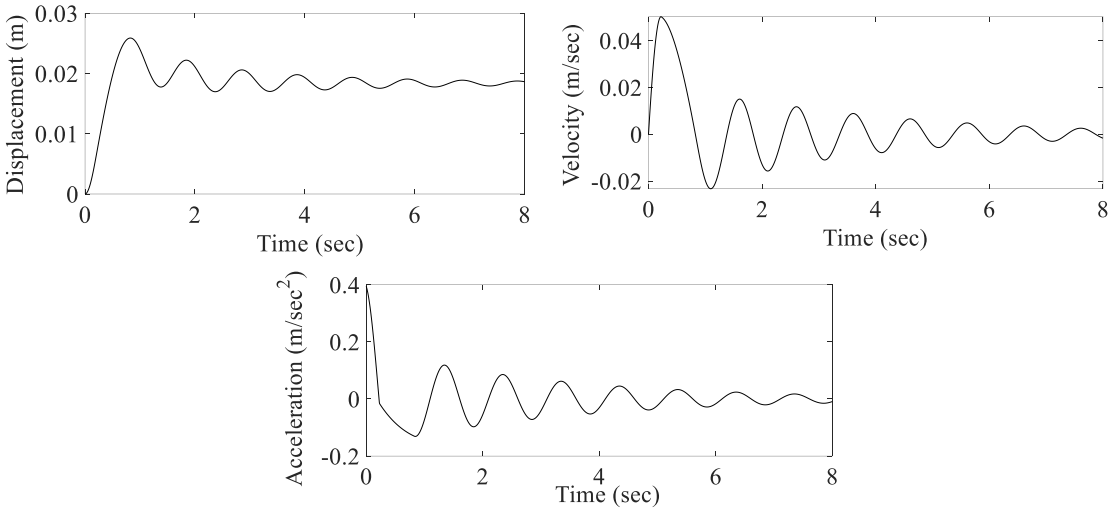

Figure 10. The displacement, velocity, and acceleration time histories of the system with full elastic-full plastic behavior subjected to the blast load with $t_d = 5\,(sec)$

According to Fig. 10, the maximum displacement, velocity, and acceleration are equal to 0.0259 (*m)*, 0.0502 (*m/sec*) and 0.3948 (*m/sec*^{2}), respectively. Also, the maximum ductility value is equal to $\mu = \frac{x_{max}}{x_y} = 3.45$. Also, Fig. 11 depicts the internal force concerning the displacement of the studied system.

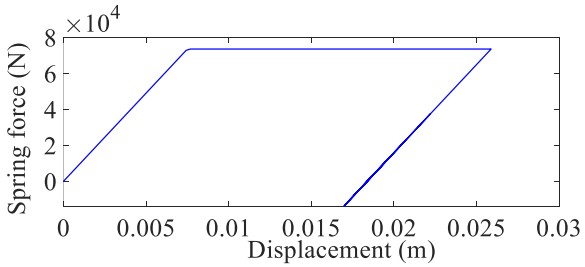

Figure 11. The change of internal force with respect to the displacement of the system subjected to the blast load with $t_d = 5\,(sec)$

The single-degree of freedom system discussed in the previous section is now re-examined. The ratio of the secondary stiffness to the primary stiffness of the system is assumed to be 0.1. The blast load on the system is also considered according to three predefined modes (impact duration 0.5 *sec*, 1.5 *sec*, and 5 *sec*). For the considered cases, the changes in internal force with respect to the displacement of the system are drawn in Fig. 12.

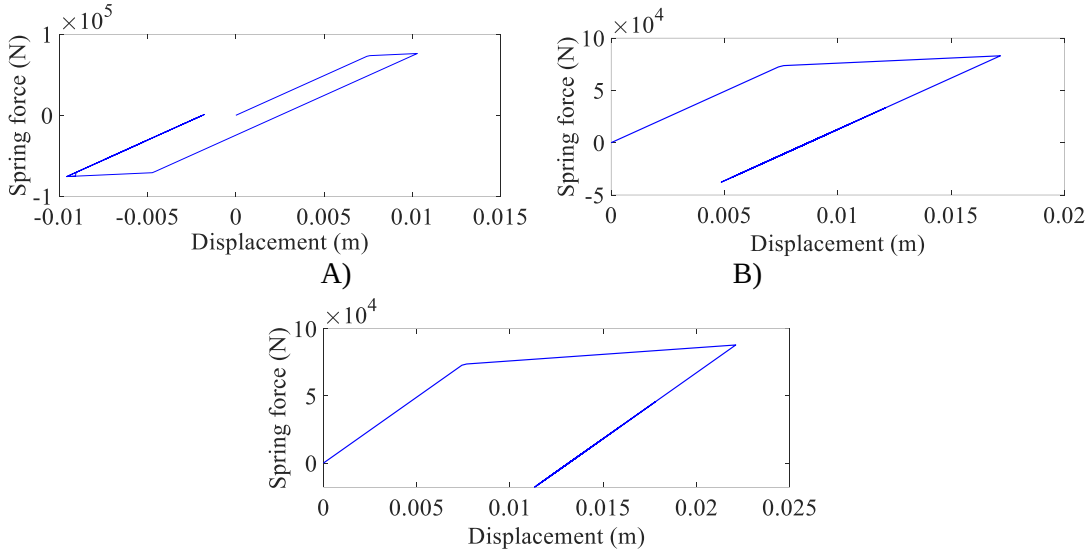

Figure 12. The change of internal force with respect to the displacement of the system subjected to the blast load with A) $t_d = 0.5\ (sec)$, B) $t_d = 1.5\ (sec)$, and C) $t_d = 5\ (sec)$ when the strain hardening is considered

Based on Fig. 12, it is clear that the shorter value for the positive impact duration of the blast load will lead to more internal force and, therefore, in this state, the system enters more into the nonlinear region. Table 1 also shows the maximum values of displacement, velocity, acceleration, and the ratio of maximum displacement to yield displacement for the elastic-plastic system with strain hardening under different blast loads.

Table 1: A comparison between the maximum response of the system subjected to the blast load with different positive phase durations

$t_d = 5\ (sec)$	$t_d = 1.5\ (sec)$	$t_d = 0.5\ (sec)$	Different loading modes
0.0221	0.0172	0.0103	$x_{\max}(m)$
0.0502	0.0471	0.0515	$\dot{x}_{\max}\ (m/\sec)$
0.3948	0.3948	0.3948	$\ddot{x}_{\max}\ (\mathrm{m/sec^2})$
2.95	2.29	1.37	$\mu = \frac{x_{\max}}{x_y}$

The results show that for the system with elastic-plastic behavior, while the strain hardening has been considered, the maximum displacement and ductility of the system increase when the duration of positive impact and, therefore, the amount of positive impact increase. The results also show that for different positive impacts, the maximum acceleration of the system remains constant, subject to the different positive impact duration.

By comparing the results of the two behavior (i.e., elastic-plastic behavior with and without considering the strain hardening), it is clear that the strain hardening has decreased the ductility. The results also show that the amount of reduction of this parameter increases with increasing the duration of the positive phase of the explosion (see Table 2).

Table 2: A comparison between the maximum ductility of the structure under blast load with different positive phase durations

$t_d = 5\ (sec)$	$t_d = 1.5\ (sec)$	$t_d = 0.5\ (sec)$	$\mu = \frac{x_{max}}{x_y}$
3.45	2.46	1.38	**Without Strain hardening**
2.95	2.29	1.37	**With Strain hardening**

This section examines two real examples to study the effect of the positive duration of blast load on the real structure. Fig. 13 shows an elevated water tank. This structure is known as a single degree of freedom system when it is full of water. The natural vibration period of the system is 0.25 *sec*, and its damping is considered equal to 5% ($\xi = 0.05$). The mass of the structure is also equal to m = 10000 ($N.sec^2 / m$). The behavior of the system is nonlinear when it is subjected to an explosive shock load with the equation $P(t) = 98100 \times (1 - \frac{t}{t_d}) \times e^{-(\frac{5t}{6})}$ in the unit of N. The yield displacement of the structure is equal to 0.01 m. Table 3 shows the maximum displacement, velocity, acceleration, and ductility of the structure for the elastic-plastic system with and without strain hardening subjected to the different blast loads.

Table 3: A comparison between the maximum response of elevated water tank subjected to the blast load with different positive phase durations

$t_d = 5\ (sec)$	$t_d = 1.5\ (sec)$	$t_d = 0.5\ (sec)$	Different loading modes	
0.08	0.07	0.049	x_{max} (m)	With strain hardening
0.40	0.38	0.34	$\dot{x}_{max}$ $(m/\sec)$	
9.81	9.81	9.81	$\ddot{x}_{max}$ (m/sec^2)	
7.81	6.84	4.88	$\mu = \frac{x_{max}}{x_y}$	

0.25	0.16	0.07	$x_{\max}$ (m)	Without strain hardening
0.52	0.45	0.35	$\dot{x}_{\max}$ $(m/\sec)$	
9.81	9.81	9.81	$\ddot{x}_{\max}$ $(\mathrm{m/sec^2})$	
25.19	15.87	7.11	$\mu = \frac{x_{\max}}{x_y}$	

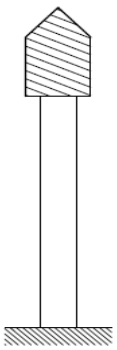

Figure 13. An elevated water tank with nonlinear behavior

In another example, a shear frame with nonlinear behavior (see Fig. 14) is considered subject to the blast load with the equation $P(t) = 20 \times (1 - \frac{t}{t_d}) \times e^{-(\frac{5t}{6})}$ in the unit of *kips*. In this example, the system damping is considered equal to $\xi =$ 0.087, and also, the natural period of the structure is 0.8 *sec*. Also, the yield displacement of the structure is considered equal to 0.75 *in*. Table 4 shows the maximum displacement, velocity, acceleration, and ductility of the structure for the elastic-plastic system with and without strain hardening behavior subjected to the different loads.

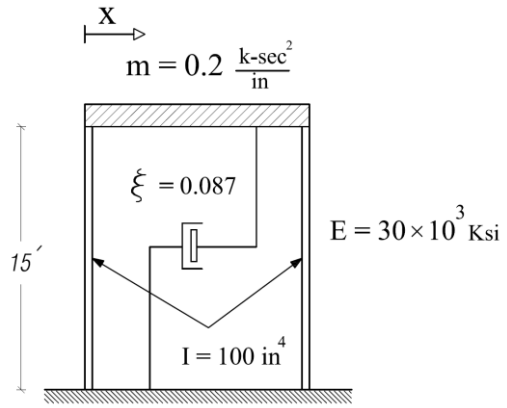

Figure 14. One-story shear frame with nonlinear behavior

Table 4: A comparison between the maximum response of shear building subjected to the blast load with different positive phase durations

$t_d = 5\ (sec)$	$t_d = 1.5\ (sec)$	$t_d = 0.5\ (sec)$	Different loading modes	
6.05	4.59	3.27	$x_{\max}$ (in)	With strain hardening
11.58	10.32	8.21	$\dot{x}_{\max}$ $(in/\sec)$	
100	100	100	$\ddot{x}_{\max}$ $(\text{in}/\sec^2)$	
8.06	6.12	4.36	$\mu = \frac{x_{\max}}{x_y}$	
10.99	6.55	9.03	$x_{\max}$ (in)	Without strain hardening
13.00	10.89	8.22	$\dot{x}_{\max}$ $(in/\sec)$	
100	100	100	$\ddot{x}_{\max}$ $(\text{in}/\sec^2)$	
14.65	8.73	12.04	$\mu = \frac{x_{\max}}{x_y}$	

The results show that for the system with elastic-plastic behavior, while the strain hardening has been considered, the maximum displacement and ductility of the system increase when the duration of positive impact and, therefore, the amount of positive impact increase. The results also show that for different positive impacts, the maximum acceleration of the system remains constant, subject to the different positive impact duration.

By comparing the results of the two behavior (i.e., elastic-plastic behavior with and without considering the strain hardening), it is clear that the strain hardening has decreased the ductility. The results also show that the amount of reduction of this parameter increases with increasing the duration of the positive phase of the explosion (see Tables 3 and 4).

4. CONCLUSIONS

This paper investigates the response of a single-degree-of-freedom system with an elastic-plastic nonlinear behavioral model, including displacement, velocity, acceleration, and ductility of the structure under blast load for different positive phase durations. The results show that for a system with full elastic-plastic behavior, increasing the duration of positive impact and the amount of positive impact on the system, the maximum displacement of the system and consequently the ratio of maximum displacement to the yield displacement of the structure increases. The results also show that for different positive phase duration, the maximum acceleration of the system with constant elastic-plastic behavior remains constant under the blast load. It should be noted that the strain hardening causes the value of ductility. However, the percentage reduction of this parameter has increased with increasing the duration of the positive phase of the blast load. Finally, it can be concluded that studying the

structure's behavior and calculating its response under the blast load, considering a more realistic model, will lead to more accurate results.

REFERENCES

1. Brode HL. Numerical solution of spherical blast waves, *J Appl Phys* 1995; **26**: 766-75.
2. Henrych J. *The Dynamics Of Explosion And Its Use*, Elsevier Science Publisher, New York, 1979.
3. Kingery CN, Bulmash G. Air Blast Parameters From TNT Spherical Air Blast And Hemispherical Surface Blast, Technical Report ARBRL-TR-02555, US Armament Research and Development Centre, Ballistic Research Laboratory, Aberdeen Proving Ground, MD, 1984.
4. Smith PD, Hetherington JG. *Blast And Ballistic Loading Of Structures*, Butterworth Heinemann, Oxford, 199
5. Kaveh A, Zakian P. Improved GWO algorithm for optimal design of truss structures, *Eng with Comput* 2018; **34**; 685-707.
6. Zakian P, Kaveh A. Topology optimization of trusses considering static and dynamic constraints using the CSS, Appl Soft Comput 2013; **13**: 2727-34.
7. Kaveh A, Fahimi Farzam M, Maroofiazar R. Comparing H2 and H∞ algorithms for optimum design of tuned mass dampers under near-fault and far-fault earthquake motions, *Period Polytech Civil Eng* 2020; **64**: 828-44.
8. Kaveh A, Aghakouchak AA, Zakian P. Reduced record method for efficient time history dynamic analysis and optimal design, *Earthq Struct* 2015; **8**: 639-63.
9. Ngo T, Mendis P, Gupta A. Blast loading and blast effects on structures – An overview, *Ramsay EJSE Special Issue: Load Struct* 2007, **7**: 76-91.
10. Chang SY. Improved numerical dissipation for explicit methods in pseudo-dynamic tests, *J Earthq Eng Struct Dyn* 1997; **26**, 917-29.
11. Chang SY. A new family of explicit methods for linear structural dynamics, *J Comput Struct* 2010; **88**: 755-72.
12. Chung J, Lee JM. A new family of explicit time integration methods for linear and non-linear structural dynamics, *Int J Numer Meth Eng* 1994; **37**: 3961-76.
13. Mullen R, Belytschko T. An analysis of an unconditionally stable explicit method, *J Comput Struct* 1983; 16: 691-6.
14. Hilber HM, Hughes TJR, Taylor RL. Improved numerical dissipation for time integration algorithms in structural dynamics, *J Earthq Eng Struct Dyn* 1977; **5**: 283-92.
15. Houbolt JC. A recurrence matrix solution for the dynamic response of elastic aircraft, *J Aero Scien* 1950; **17**: 540-50.
16. Newmark NM. A method of computational for structural dynamics, *J Eng Mech* 1959; **85**: 67-94.
17. Park KC. An improved stiffly stable method for direct integration of nonlinear structural dynamic equations, *J Appl Mech* 1975; **42**: 464-70.
18. Ebeling RM, Green RA, French SE. Accuracy Of Response Of Single-Degree-Of-Freedom Systems To Ground Motion, U. S. Army Corps of Engineers, Technical Report ITL-97-7; 1977.

19. Dokainish MA, Subbaraj K. A survey of direct time integration methods in computational structural dynamics. I. explicit methods, *J Comput Struct* 1989; **32**: 1371-86.
20. Dokainish MA, Subbaraj K. A survey of direct time integration methods in computational structural dynamics. II. implicit methods, *J Comput Struct* 1989; **32**: 1387-1401.
21. Kamgar R, Rahgozar R. a simple method for determining the response of linear dynamic systems, *Asian J Civil Eng* 2016; **17**: 785-801.
22. Rostami S, Kamgar R. insight to the newmark implicit time integration method for solving the wave propagation problems, *Iran J Sci Technol, Transact Civil Eng* 2022, **46**: 679-97.
23. Chang SY. Explicit pseudo-dynamic algorithm with unconditional stability, *J Eng Mech* 2009; **128**: 935-47.
24. Clarence WS. *Vibration And Shock Handbook*, CRC Press, Taylor & Francis Group, New York, 2005.
25. Indian Standard Criteria For Blast Resistant Design Of Structures For Explosions Above Ground (3rd Report), 1993.
26. Amini M, Shojaee S, Rosrami S. Inelastic dynamic analysis of structures under blast loads using generalized b-spline method, *Asian J Civil Eng* 2015; **16**: 183-202.
27. Tavakoli R, Kamgar R, Rahgozar R. The best location of belt truss system in tall buildings using multiple criteria subjected to blast loading, *Civil Eng J* 2018; **4**: 1338-53.
28. Kamgar R, Shams GR. Effect of blast load in nonlinear dynamic response of the buckling restrained braces core, *Adv Defense Sci Technol* 2018; **9**: 107-118 (In Persian).
29. Kamgar R, Majidi N, Heidarzadeh H. Optimum layout of mega buckling-restrained braces to optimize the behavior of tall buildings subjected to blast load, *Adv Defense Sci Technol* 2020; **2**: 211-30 (In Persian).
30. Kamgar R, Askari Y, Majidi N. The effect of blast load and earthquake load on the nonlinear behavior of structures, *Bull Earthq Sci Eng* 2020; **7**: 119-32 (In Persian).
31. Fazlavi M, Asadian AA. Evaluation of changing effects of density and thickness of polyurethane as a protective coating on underground tunnels under surface blast, *Karafan* 2021; **18**: 119-34 (In Persian).
32. Magnussa NM, Morrill K. Fast running model for the residual capacity of steel columns damaged by blast and fragment loads, *Proccedings of the 79th Shock and Vibration Symposium* 2008, Orlando, FLorida.
33. Boheiraee M, Biglari M, Ashayeri I. Numerical assessment of explicit dynamic analysis of structures in severe loading (Case study of three concrete slabs), *Bull Earthq Sci Eng* 2015; **2**: 13-23 (In Persian).
34. Habibi AR, Khaledy N. Evaluating rectangular loading pattern in nonlinear analysis of composite bridges under blast, *Asian J Civil Eng* 2015; **26**(2): 67-84.
35. Khaledy N, Habibi A, Memarzadeh P. A comparison between different techniques for optimum design of steel frames subjected to blast, *Latin American J Solid Struct* 2018, **15**(9): e106.
36. Khaledy N, Habibi A, Memarzadeh P. Minimum weight and drift design of steel moment frames subjected to blast, *Int J Optim Civil Eng* 2019; **9**(1): 39-63.

37. Mondal PD, Ghosh A, Chakraborty S. Fluid viscous damper in mitigation of structural vibration effect due to underground blast, *Int J Mat Struct Int* 2014; **8**(4): 273-90.
38. Mondal PD, Ghosh AD, Chakraborty S. Performances of various base isolation systems in mitigation of structural vibration due to underground blast induced ground motion; *Int J Struct Stab Dyn* 2017; **17**(04): 1750043.
39. Kangda MZ, Bakre, S. The effect of lrb parameters on structural responses for blast and seismic loads, *Arab J Sci Eng* 2018; **43**(4): 1761-76.
40. Zhang R, Phillips BM. Performance and protection of base-isolated structures under blast loading, *J Eng Mech* 2016; **142**(1): 04015063.
41. Zhang Ch, Gholipour Gh, Mousavi AA. Blast loads induced responses of rc structural members: state-of-the-art review, *Comp Par B: Eng* 2020; **195**: 108066.
42. Gholipour Gh, Zhang Ch, Mousavi AA. Numerical analysis of axially loaded RC columns subjected to the combination of impact and blast loads, *Eng Struct* 2020; **219**: 110924.
43. Peymani Forushani S, Hoseini SA. SDOF system solution of the two-way RC slab subjected to blast loading, *Adv Defense Sci Technol* 2021; **12**(2): 185-96 (In Persian).
44. Clough R, Penzien J. *Dynamics of Structures*, McGraw-Hill, USA, 2003.